VOL. 21, NO. 5, MARCH 2026 ISSN 1819-6608
ARPN Journal of Engineering and Applied Sciences

www.arpnjournals.com

OPTIMIZATION OF ADDITIVE MANUFACTURING PARAMETERS TO ENHANCE STRENGTH AND SURFACE QUALITY IN HYBRID ABS-CARBON FIBER 3D PRINTED COMPONENTS

Sathish T.
Department of Mechanical Engineering, Saveetha School of Engineering, Saveetha Institute of Medical and Technical Sciences, Chennai, Tamil Nadu, India
E-Mail: sathisht.sse@saveetha.com

ABSTRACT

Lightweight composite printing is highly demanded for precision and lightweight solutions. This work focuses on enhancing the strength and surface quality of FDM-3D printed hybrid composite parts. Fused Deposition Modelling (FDM) is one of the techniques for producing components with superior strength while keeping the required geometric accuracy. In this research work, Acrylonitrile Butadiene Styrene (ABS) and composite materials, namely carbon fiber filaments, were chosen for fabricating 3D-printed parts. Unlike conventional approaches using homogeneous composite filaments, this research adopts a novel layer-by-layer strategy, alternating between pure ABS and carbon fiber material to create a hybrid structure. The primary objective of this work is to examine and maximize the compressive strength and minimize the surface roughness of these 3D-printed components. To attain this, the Taguchi Design of Experiments method was used with L16 type Orthogonal Array to statistically examine various parameter combinations. Four different key 3D printing process parameters were chosen for optimization, each with four levels of this work Parameters are namely, Nozzle Diameter (0.2, 0.4, 0.6, and 0.8 mm), Printing Speed (30, 40, 50, and 60 mm/sec), Layer Thickness (0.1, 0.15, 0.2, and 0.25 mm), and Nozzle Temperature (210°C, 220°C, 230°C, and 240°C). The results of this investigation discovered that the maximum compressive strength attained was 38 MPa, while the minimum surface roughness recorded was 2.839 microns. In both results, similar parameter levels and values were effects like as 0.8 mm of nozzle diameter, 50 mm/sec of printing speed, 0.15 mm of layer thickness, and nozzle temperature of 240°C.

Keywords: bi-layered printing, parameter optimization, lightweight, composite, local materials, sustainable.

Manuscript Received 22 January 2026; Revised 13 March 2026; Published 10 May 2026

1. INTRODUCTION

Because industrial manufacturing is advancing fast, many components now require very accurate sizes and complex shapes that are normally hard to produce reliably using traditional metal and alloy techniques. Beginning with CAD models and building parts directly one layer at a time by 3D printing, AM allows the construction of parts from different materials such as metals and polymers [1, 2]. Because of this technology, production can now create complex and custom options with amazing precision in many fields [3].

In the past few years, AM has seen great success as a way to manufacture difficult or impossible parts that are not easily fabricated with traditional tools [4]. Composites are more valuable in aerospace and marine industries partly because they can generate both strong and lightweight parts [5]. There is a wide range of advanced techniques in AM, each developed to fulfil certain manufacturing needs. Among the main methods used are Direct Metal Laser Sintering (DMLS), Stereolithography (SLA), Selective Laser Sintering (SLS), Selective Laser Melting (SLM), Electron Beam Melting (EBM), and Digital Light Processing (DLP). Materials, energy use, and part complexity are different for each of these fabrication technologies [6-8]. High-strength metal pieces are best made with DMLS and SLM, while SLA and DLP are the best for making plastic or polymer parts with many details [9].

Many AM users prefer Fused Deposition Modelling (FDM) because it is simple to use, cost-effective, and versatile. Many industries, such as automotive, aerospace, and consumer goods, prefer FDM because it makes it easy to create both useful prototypes and finished parts using various thermoplastics [10-12].

The quality of FDM continues to grow as advances in material science and printing techniques grow its applications, making it a key player in the approach to manufacturing. The increasing trust in Additive Manufacturing, especially in critical industries like marine and aerospace, exhibits its transformative impact on modern production. As new technologies and materials proceed to develop, AM is set to play an even more important role in shaping the future of manufacturing, offering greater efficiency, flexibility, and innovation [13, 14]. Fused Deposition Modelling (FDM) stands out as one of the most widely adopted technologies for 3D printing. The FDM process works by heating and melting filament materials, which are then exactly deposited in layers to shape the desired product. This shape is pre-defined in the CAD model, assuring accuracy and consistency in the final product. Several types of filament materials are normally used in FDM 3D printing, each providing unique properties suited to different applications [15-17]. These

materials are considered as Acrylonitrile Butadiene Styrene (ABS), Polylactic Acid (PLA), Polycarbonate (PC), Polymethyl Methacrylate (PMMA), Polyethylene (PE), Nylon, Polyethylene Terephthalate Glycol (PETG), and Polypropylene (PP). Each material conveys its own pros in terms of strength, flexibility, durability, or resistance to environmental factors [18]. This skilfulness has made FDM one of the most sought-after disciplines for producing functional parts across a wide range of industries, from automotive and aerospace to healthcare and user products. As the need for complex and fine products continues to rise, the function of Additive Manufacturing, especially FDM, will only develop in value. Its ability to quickly produce elaborate and customized parts makes it a priceless tool in recent industrial production [19-21]. Fused Deposition Modelling (FDM) operates by depositing a heated filament layer by layer to make a 3D object. In this process, the filament is heated and extruded through a nozzle, with all layers being deposited consecutively. After forming each layer, the extruder head moves up, allowing for the adjacent layer to be added, and this continues until the whole object is completed [22-25]. The filaments utilized in FDM are typically thermoplastics and come in round, wire-like shapes. These filaments are fed through with guides into a preheated extruder, which utilizes a stepper motor to drive the gear execution, known as the extruder motor. As the filament passes through the extruder, it is heated to a molten state and then comes out through a brass nozzle. The nozzle deposits the melted filament onto the print bed, where each layer of the model is stacked upon the previous one [26-29]. The motion of the extruder and the speed of the printing process are monitored and controlled by stepper motors, guaranteeing precision and accuracy. For example, when using Acrylonitrile Butadiene Styrene (ABS) as the filament material, the print bed is heated to approximately 100°C, while for Polylactic Acid (PLA), the bed temperature is maintained at 60°C. This controlled heating assist ensures proper adhesiveness of the layers and prevents deformation of the printed object [30-32].

FDM printing is highly respected for its ability to produce parts with superior dimensional accuracy and strength. In addition to these benefits, the FDM process provides various advantages, including low material and operational costs, speedy fabrication times, low energy intake, and minimum material wastage. These qualities make it an attractive quality for prototyping and manufacturing in different industries [33-35]. One of the key factors that powers the final result of FDM-printed parts is the selection of printing parameters. Parameters such as nozzle temperature, layer thickness, print speed, and bed temperature employ a critical role in determining the mechanical properties, surface finish, and total quality of the printed components [36]. Adjusting these parameters allows manufacturers to optimize the execution and functionality of their 3D-printed parts, making FDM a variable and adaptable technology for a wide range of applications. The statistical approach known as the Taguchi design of experiments furnishes an effective and reliable method for optimizing different process parameters in manufacturing and research [37]. By consistently varying the process parameters, this approach modifies the identification of the optimal settings that lead to the most possible outcomes. One of the key advantages of the Taguchi method is its ability to find robust solutions that minimize modification and improve product quality, even when multiple factors are employed. In addition to furnishing an optimal solution, the Taguchi design of experiments also provides insight into the influence of each parameter on the results [38, 39]. This is often increased by analysis using Analysis of Variance (ANOVA), which assist quantify the effort of each factor in the experimental work. ANOVA breaks down the variability in the experimental data to reveal which process parameters have the most important impact on the desired outcomes. By doing so, it helps researchers and engineers realize which factors are critical and which can be tuned without significantly affecting the results. Overall, the accumulation of the Taguchi method and ANOVA creates a powerful statistical framework for enhancing process efficiency and achieving desired outcomes with exactness [40]. It allows for a systematic and data-driven conceptualization of experimentation, making it a valuable tool in fields ranging from manufacturing to product improvement and beyond. This approach not only assist optimize performance but also assures that the solutions are robust and trustworthy under varying conditions [41]. The novelty of this investigation and the research gap analysis were presented in Table-1.

Table-1. Research Gap Analysis.

Ref. No.	Reference	Material & Method	Key Findings	Identified Research Gaps	Novelty of Current Study
[1]	Saharudin *et al*. (2020)	PLA and PA reinforced with carbon fibers using FDM and CFF	Evaluated surface texture and mechanical properties; noted differences between FDM and CFF techniques.	Limited to PLA and PA matrices; did not explore ABS-carbon fiber composites.	Investigates ABS-carbon fiber composites, expanding material scope beyond PLA and PA.
[5]	Agarwal *et al*. (2022)	ABS specimens via FDM	Analyzed the impact of print parameters on dimensional variation; identified optimal settings for dimensional accuracy.	Focused on dimensional accuracy; lacked analysis of mechanical strength and surface quality.	Emphasizes both mechanical strength and surface quality in ABS-carbon fiber composites.
[10]	Maqsood & Rimašauskas (2021)	Carbon fiber reinforced PLA via FDM	Characterized mechanical properties; observed improvements with carbon fiber addition.	Did not assess surface roughness or optimize process parameters.	Incorporates surface roughness analysis and parameter optimization using the Taguchi method.
[16]	Saleh *et al*. (2022)	Carbon fiber/PLA composite lattice structures	Predicted mechanical properties using mathematical and ANFIS models; validated with experiments.	Focused on lattice structures; did not explore solid components or ABS-based composites.	Targets solid ABS-carbon fiber components, providing insights beyond lattice structures.
[18]	Dou *et al*. (2019)	Continuous carbon fiber-reinforced PLA via modified FDM	Studied the effect of process parameters on tensile properties; highlighted the importance of layer height and extrusion width.	Concentrated on tensile properties; lacked compressive strength and surface quality analysis.	Evaluates compressive strength and surface roughness, offering a more comprehensive assessment.
[24]	Kumar *et al*. (2024)	PLA with carbon nanofiber addition via FDM	Reported enhanced mechanical properties with 3% carbon nanofiber addition.	Did not investigate ABS matrices or surface quality aspects.	Explores ABS-carbon fiber composites, including surface quality evaluation.
[27]	Kamaal *et al*. (2021)	Carbon fiber–PLA composites via FDM	Examined the effect of process parameters on mechanical properties; identified optimal settings for tensile strength.	Focused on PLA composites; did not assess ABS-carbon fiber materials or surface roughness.	Investigates ABS-carbon fiber composites with emphasis on surface roughness optimization.
[29]	Khalili *et al*. (2023)	PLA/Continuous carbon fiber composites via FDM	Analyzed tensile and flexural properties; demonstrated improvements with continuous fibers.	Did not consider ABS matrices or surface quality metrics.	Provides insights into ABS-carbon fiber composites, including surface roughness analysis.
[31]	Arunkumar *et al*. (2021)	PLA and PA with carbon additives via 3D printing	Studied mechanical properties; noted enhancements with carbon additives.	Limited to PLA and PA; lacked focus on ABS-carbon fiber composites and surface quality.	Expands research to ABS-carbon fiber composites with surface quality considerations.
[34]	Chawla *et al*. (2023)	Recycled ABS-based composites via FFF	Investigated mechanical properties; highlighted potential of recycled materials.	Did not explore carbon fiber reinforcement or surface roughness optimization.	Focuses on virgin ABS-carbon fiber composites with surface quality enhancement.
[36]	Thakur *et al*. (2023)	PLA-carbon fiber-PLA sandwiched composites via hybrid AM	Optimized mechanical properties using machine learning; demonstrated sustainability aspects.	Emphasized sustainability; did not assess ABS-carbon fiber composites or surface roughness.	Concentrates on ABS-carbon fiber composites with surface quality optimization.
[42]	Khan *et al*. (2023)	PLA-PETG-ABS tri-material composites via FFF	Investigated mechanical properties; optimized process parameters for impact	Focused on tri-material composites; lacked specific analysis of ABS-	Provides targeted analysis of ABS-carbon fiber composites with

			strength.	carbon fiber combinations.	parameter optimization.
[43]	Khan *et al*. (2024)	Multi-material polymeric laminated structures via extrusion-based AM	Reviewed advancements in multi-material AM; discussed challenges and opportunities.	Offered a broad review; did not provide experimental data on ABS-carbon fiber composites.	Delivers experimental insights into ABS-carbon fiber composites, addressing identified gaps.
[44]	Khan *et al*. (2025)	Thick tri-material layered composites via extrusion-based AM	Studied effects of processing parameters on impact strength and microstructure.	Concentrated on tri-material systems; did not explore ABS-carbon fiber composites specifically.	Focuses on ABS-carbon fiber composites with detailed parameter optimization.
[45]	Khan *et al*. (2025)	Carbon particle-reinforced TPU via FFF	Optimized processing parameters to enhance mechanical properties; utilized the design of experiments.	Investigated TPU matrices; did not assess ABS-carbon fiber composites or surface quality.	Applies design of experiments to ABS-carbon fiber composites, including surface quality analysis.
[46]	Abas *et al*. (2025)	Carbon fiber-reinforced PLA via extrusion-based AM	Employed a definitive screening design to enhance mechanical properties; identified key parameters.	Focused on PLA matrices; lacked exploration of ABS-carbon fiber composites and surface roughness.	Implements parameter optimization for ABS-carbon fiber composites with surface quality focus.

Even though printing with ABS and carbon fiber filament is possible in the market, this study aims to find a fresh way of printing that goes beyond just mixing materials. The research briefly presents a technique in which FDM printing alternately deposits whole ABS and carbon fiber composite hybrid layers / bi-layers. Such structuring makes it possible to manage the internal order of the part, increasing its strength and the quality of its outside finish [42]. The idea is that by varying the pattern and characteristics of the layers, features that are not possible with homogeneous composite filaments can be achieved. In this study, the nozzle diameter, printing speed, layer thickness, and nozzle temperature are carefully selected to optimize strength and improve the surface quality of the printed parts. By customizing the optimization based on different printing processes, the model clearly shows how changing printing parameters can affect the function and quality of the structure, which is in line with the requirements of advanced engineering.

The primary objective of this work is to produce 3D-printed parts using a hybrid bi-layered filament composed of ABS and carbon fiber. These parts are manufactured through the Fused Deposition Modelling (FDM) method, and the process parameters are optimized using the Taguchi statistical approach. Finally, the printed parts are tested to measure their compressive strength and surface roughness.

2. MATERIALS AND METHODS

In this investigation, two different filaments, namely Acrylonitrile Butadiene Styrene (ABS) and Carbon fiber, were employed to print the single part. ABS has better rigidity and resilience to wear and abrasion, high impact, and strain properties [43]. Numerous products can be produced with the use of ABS pipe fittings, toys, electronics panels, and structural applications [44]. Another material is carbon fiber, which possesses high stiffness and strength, offers dimensional accuracy, and heat and flame resistance [45, 46]. Both filaments were procured from 3D Print World Private Limited, Mumbai, with a 1.75 mm diameter. 3D printing was conducted by Fused Deposition Modelling (FDM), which offered a continuous filament supply with selected temperature levels. Printing is conducted layer by layer with two different filaments alternatively, which increases the strength of the prints.

3. EXPERIMENTAL PROCEDURE

3D printing process was conducted through Model: Ender 5 Plus 3D printer with printing size of dimensions of 350 mm x 350 mm x 400 mm. The printing speed of that machine was 100 mm/sec, and the slice thickness was 0.1 mm to 4 mm. The hybrid, like a bi-layered composite, was prepared by using slicing software and printers. Here, in the single extruder head setup, two nozzles were used for printing of ABS and carbon fiber filaments; two extruders are used to feed the ABS and carbon filament separately, alternately to form a bi-layered 3D printing part as shown in Figure 1. It was achieved by, at that time, one extruder delivered one filament, then another one. Slicing of the specimen was done by using CAD model software, namely Cura 3D software, it fed into the Enter 5 plus 3D printer machine. The Taguchi approach was implemented to conduct the 3D printing process with sixteen sets of experimental runs for compressive strength and surface roughness analysis. 3D printing was carried out with selected parameters like Nozzle diameter 0.2, 0.4, 0.6, and 0.8 mm, printing speed 30, 40, 50, and 60 mm/sec, layer thickness 0.1, 0.15, 0.2, and 0.25 mm, and nozzle temperature 210°C, 220°C, 230°C, and 240°C. Raster angle maintained as $^{0^\circ}$ with flat build orientation, infill density is 100 %, then 80°C

platform temperature was maintained for all prints. Both extruders simultaneously extrude a bi-layered thickness of ABS and carbon fiber filaments. The dimensions of the 3D printed parts were 100 mm x 100 mm x 20 mm.

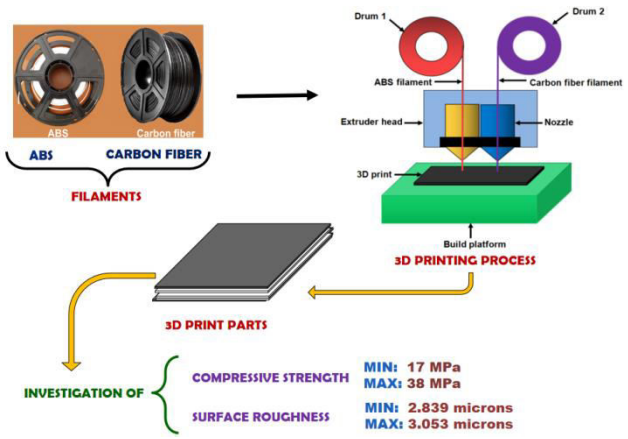

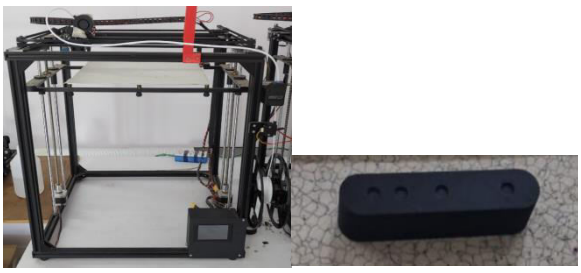

Figure-1. Experimental flow diagram and actual 3D printing setup with printed part.

There were sixteen specimens printed as per the ASTM D695 standard for conducting compressive strength, and another sixteen specimens were printed for conducting surface roughness analysis. The dimensions of the compressive strength specimens are 25 mm x 13 mm x 13 mm. Compressive strength was analysed by using a Computer-Controlled Electronic Universal Testing Machine. For polymer-based composites such as ABS reinforced with carbon fibers, the standard reference is ASTM D695, which specifies a constant crosshead speed of 1.3 mm/min for testing the compressive properties of rigid plastics. The same was followed.

Similarly, the surface roughness specimens are prepared as 80 mm x 50 mm x 5 mm. The surface roughness was measured through a surface analyzer with the SURFCOM TOUCH 50. The surface measurement was conducted twice, and the average readings were considered for analysis.

Table-2. 3D printing process parameters and their levels

S. No	Parameters	Level 1	Level 2	Level 3	Level 4
1.	Nozzle Diameter (mm)	0.2	0.4	0.6	0.8
2.	Printing speed (mm/sec)	30	40	50	60
3.	Layer thickness (mm)	0.1	0.15	0.2	0.25
4.	Nozzle temperature (^{0}C)	210	220	230	240

The main key parameters and their levels of the 3D printing process were presented in Table-2; they were named as nozzle diameter, printing speed, Layer thickness, and nozzle temperature. Different combinations of parameters affect the compressive strength and surface roughness of 3D printed parts. FDM process settings were decided according to what was described in the manufacturer's catalogue, following the pre-test. Nozzle diameters tested ranged from 0.2 mm to 0.8 mm. A narrower diameter (0.2 mm) makes the prints detailed and smooth, yet it can make the printer clog when filaments contain many fibers. Industries usually use 0.4 mm nozzles, which give a decent mix of extrusion and detail quality. Zero six (0.6) and zero eight (0.8) mm nozzles let you deposit material at a higher rate and are best for composites with carbon fibers, helping to avoid clogging and secure good print results [21]. The software was used to print at speeds of 30 mm/sec and 60 mm/sec to understand how print time and part outcome are related. Lowering the extrusion rate (Velocity) to 30 mm/sec improves bonding between layers and prevents the creation of weak voids. At 40-50 mm/sec, typical printing for a prototype can be done, but moving up to 60 mm/sec lets you measure the top limits of quality and strength, which is especially true for filaments with a fiber blend [20, 23, 44].

The layers measured from 0.1 mm to 0.25 mm in thickness. When the layer thickness is 0.1 mm, the surface looks better, and the layers are more tightly held together, though it slows down the printing. A layer of 0.15 mm helps deliver good part quality without sacrificing speed; 0.2 mm brings both good speed and solid quality, while 0.25 mm produces parts more quickly but reduces surface detail and may weaken the connection between layers [6, 23, 32, 44]. The nozzle temperature was set between 210°C and 240°C during the test. Just below 210°C is the

minimum temperature required for ABS, but 220°C and 230°C lead to the best polymer flow and bonding. At a temperature of 240°C, it can be noticed that improved movement of the melt and better interactions between the fiber and polymer, though careful attention is given to avoid heat damage to the materials [7, 20, 45]. The temperature span is vital to understanding the cooling process of the carbon fiber-ABS material during extrusion. Varying the nozzle diameter (0.2 mm, 0.4 mm, 0.6 mm, and 0.8 mm) automatically changes the extrusion width, a main factor in Fused Deposition Modelling (FDM). Generally, the width of the extrusion matches the size of the nozzle, so a bigger nozzle extrudes more material at one time [21]. The extrusion width is usually broader with a 0.8 mm nozzle and narrower with a 0.2 mm nozzle. As a result, both the accuracy of the shape, the smoothness of the surface, and the strength of the layers in the printed piece can be influenced. In the study, maintaining uniform results for different nozzle diameters was achieved by increasing the width of the printing line as needed in the software settings. Adjusting the extrusion width to match the nozzle diameter, this helps to prevent uneven layers, secure proper adhesion between printing parts, and prevent too much or not enough filaments from coming out of the nozzle [21].

The standard of printed parts changed according to the nozzle diameter. Stronger and better fused layers, as well as increased compressive strength, were possible with the use of the 0.8 mm nozzle. Yet, to achieve that, the surface texture and clarity had to be slightly reduced. In contrast, using small nozzles gave high detail and good surface quality yet made the printed parts less resistant to pressure and less likely to stick well after layers. Through the Taguchi Design of Experiments approach, the extrusion width settings, as well as other parameters, were found so that both strength and surface quality were at optimal levels. With this strategy, extrusion results were controlled, and all nozzle diameters generated high-quality parts.

A fixed 100% infill and a zero raster angle were set in this investigation to reduce internal pattern variations and make the material throughout the specimen more uniform. A full infill guarantees the part is solid all around, so there is no influence from porosity or holes within the mechanics and the surface. Because of this, the impact of individual process parameters like nozzle size, printing speed, layer height, and printing temperature on the print's outcome can be analyzed more effectively. Just as 45° prevents variations in mechanical responses, 0° holds filament orientation strictly in one loading direction, meaning no differences or variations with respect to where or how the print is loaded. Limiting these factors allows the analysis to examine only the main FDM parameters, improving the accuracy of the results and making the findings meaningful for making better hybrid ABS-carbon fiber parts.

4. RESULTS AND DISCUSSIONS

In this work, the Taguchi optimization L16 orthogonal array statistical approach was used to examine the parameters with their significant effects in the investigation results.

Table-3. An elaborated experimental summary of the 3D Printing process.

Exp. Runs	Nozzle Diameter (mm)	Printing speed (mm/sec)	Layer thickness (mm)	Nozzle temperature (^{0}C)	Compressive strength (MPa)	Surface Roughness (Microns)
1	0.2	30	0.10	210	17	3.053
2	0.2	40	0.15	220	25	2.979
3	0.2	50	0.20	230	29	2.881
4	0.2	60	0.25	240	36	2.862
5	0.4	30	0.15	230	27	2.909
6	0.4	40	0.10	240	33	2.885
7	0.4	50	0.25	210	23	2.892
8	0.4	60	0.20	220	32	2.924
9	0.6	30	0.20	240	34	2.895
10	0.6	40	0.25	230	33	2.862
11	0.6	50	0.10	220	28	2.932
12	0.6	60	0.15	210	26	2.909
13	0.8	30	0.25	220	32	2.866
14	0.8	40	0.20	210	24	2.881
15	0.8	50	0.15	240	38	2.839
16	0.8	60	0.10	230	32	2.878

The outcome results of the sixteen experimental runs were illustrated in Table-3. Many of the experimental runs provided excellent results in terms of maximum compressive strength and minimum surface roughness of the 3D printed parts. Based on the different combination sets of results, the maximum compressive strength was attained as 38 MPa, and the minimum surface roughness was recorded as 2.839 microns. It was achieved with the influence of 0.8 mm of nozzle diameter, 50 mm/sec of printing speed, 0.15 mm of layer thickness, and nozzle temperature of 240°C. Higher levels of nozzle diameter and nozzle temperature offered excellent results.

4.1 Compressive Strength Analysis

In the compressive strength analysis, the nozzle temperature was highly influential in modifying the strength of the 3D parts compared to other parameters. Based on the rank order and delta value, the parameters influencing were presented in Table-4. Nozzle temperature was the high priority, like first rank, followed by nozzle diameter, second priority; it got second rank. Then printing speed was the third priority, like third rank; finally, layer thickness was the fourth priority, like fourth rank. In compressive strength analysis, the optimal parameters were recorded as 0.8 mm of nozzle diameter, 60 mm/sec of printing speed, 0.25 mm of layer thickness, and nozzle temperature of 240°C. Higher values of the parameters increased the compressive strength of the 3D printed parts.

Table-4. Compressive strength response table for signal to noise ratios.

Level	Nozzle Diameter (mm)	Printing speed (mm/sec)	Layer thickness (mm)	Nozzle temperature (^{0}C)
1	28.24	28.49	28.51	26.94
2	29.08	29.08	29.12	29.28
3	29.56	29.26	29.40	29.59
4	29.85	29.91	29.71	30.93
Delta	1.62	1.42	1.20	3.99
Rank	2	3	4	1

The The main effects plot for the Means and S/N ratios of compressive strength analysis was illustrated in Figure-2. These plots provided the parameters' position on how parameters modify the overall compressive strength of the 3D printed parts. In this plot, all the parameter values were transformed into Means and S/N ratio values, offering a clear perspective of their effect. A lower level of nozzle diameter, 0.2 mm, offered low compressive strength. Further increasing the nozzle diameter increases the compressive strength; a 0.8 mm nozzle diameter provided excellent strength. From the printing speed point of view, higher printing speed offered the next lower, higher strength, respectively.

The printing speed of 60 mm/sec recorded the extreme strength of the 3D printed parts. Similar manner in a layer thickness was observed such as 0.25 mm layer thickness offered extreme strength to the hybrid 3D printed parts. Finally, from the nozzle temperature point of view, the increasing trends of the temperature levels offered good strength at 240 ºC indicated that the excellent strength of the hybrid 3D printed parts. From this analysis, higher parameter values offered extraordinary compressive strength.

FDM 3D-printed specimen properties are strongly affected by changes in parameters such as nozzle width, printing speed, the thickness of each layer and nozzle temperature. The main effects plot for means and S/N ratios makes it obvious how every parameter influences the work well of the printed parts. Printing with thin nozzles such as 0.2 mm results in less highly compressed layers, poorer bonding and a greater possibility of forming defects in the final structure. An increase in nozzle size to 0.8 mm leads to more stable and solid material flow which improves fusion among layers and results in building denser structures. For that reason, the printer's total compression strength improves.

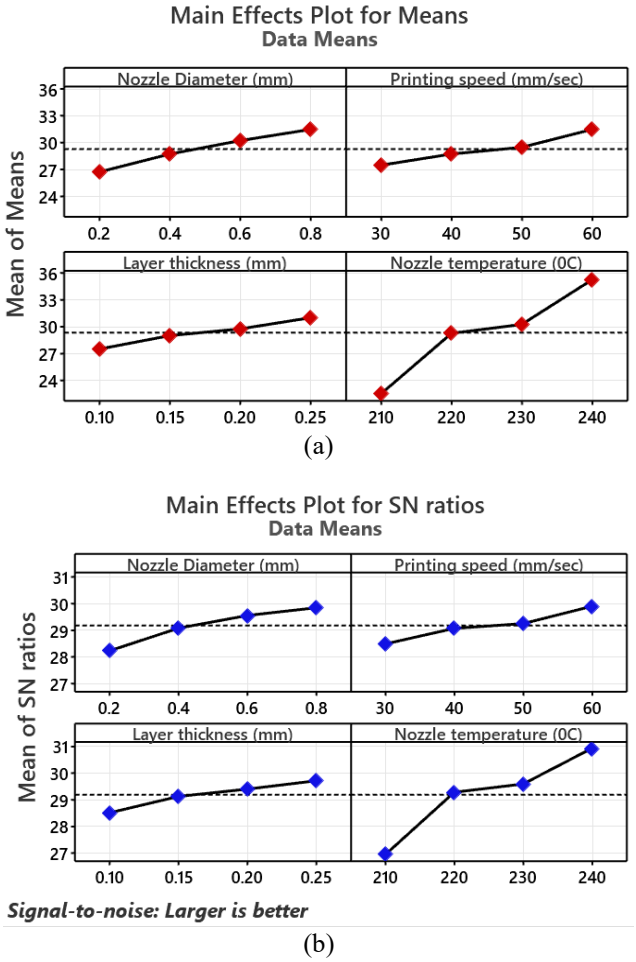

(a)

(b)

Figure-2. Compressive strength analysis main effects plot: (a) Means and (b) S/N ratio.

Slower printers give you greater control over the deposition, but this could cause the materials to heat up or build up excess, which might damage the mechanical properties of the object. When printing speed is raised to 60 mm/seconds, the faster movement helps the material be deposited and firmer before the part is produced. When the layers are thicker, such as at 0.25 mm, fewer layers need to be pressed together, making the bulky fabric's weaker points fewer and the loading more even under compression, resulting in stronger composites.

The quality of layer bonding depends greatly on nozzle temperature. As the temperature increases, up to 240°C, the polymer's flow and ability to pass between layers are enhanced, allowing adjoining sections to stick together strongly. Better bonding is a major reason why the printed parts are more resistant to compression. In short, raising every studied factor leads to a stronger compressive strength, which gives denser, more compact, and tougher structures in specimens printed from ABS and Carbon Fiber materials on an FDM printer.

The normal probability plot, as shown in Figure-3, illustrates the orientation of the sixteen experimental results. In this analysis, nearly to 80 % of the experimental results points were placed on the centre mean line that denotes selected parameters, and the conduct of the test was accurate. Only a few experimental results were deviated, that's not affect the entire experimental results.

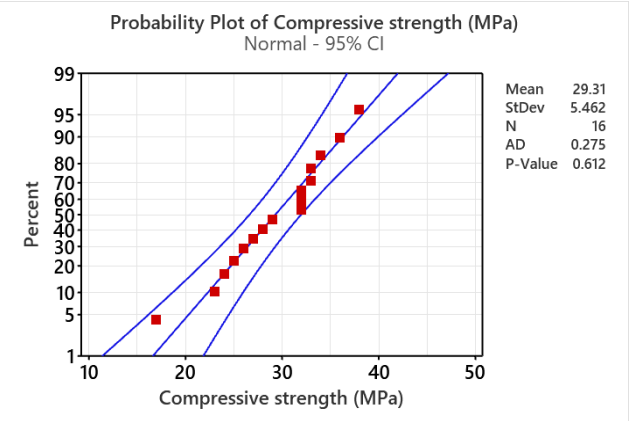

Figure-3. Normal probability plot for compressive strength analysis.

The detailed results of the ANOVA analysis for the compressive strength were tabulated in Table-5, all the parameters' contributions were clearly indicated. In this analysis, 95% confidence level was considered, and the P-value was also considered as 0.05. Based on that, all the P-values of parameters were found below 0.05. These findings clearly showed that the selected parameters and their contribution to the compressive strength analysis were statistically significant.

Table-5. Compressive strength ANOVA analysis.

Source	DF	Seq SS	Contribution	Adj SS	Adj MS	F-Value	P-Value
Regression	4	415.55	92.87%	415.55	103.888	35.84	0.000
Nozzle Diameter (mm)	1	49.61	11.09%	49.61	49.613	17.11	0.002
Printing speed (mm/sec)	1	32.51	7.27%	32.51	32.513	11.22	0.006
Layer thickness (mm)	1	25.31	5.66%	25.31	25.312	8.73	0.013
Nozzle temperature (^{0}C)	1	308.11	68.86%	308.11	308.113	106.29	0.000
Error	11	31.89	7.13%	31.89	2.899		
Total	15	447.44	100.00%				

Notification of minimum levels of P-values is reflected in the results of the compressive strength. It was achieved by a good selection of parameters, and confirmed that the compressive strength was examined accurately. Compared to the four parameters' contribution, the nozzle temperature contributed highly, such as 68.86 %. The nozzle diameter contributed 11.09 %, followed by printing speed 7.27%, and finally layer thickness contributed as 5.66 %. From this contribution, the nozzle plays a vital role in terms of its diameter and operating temperature.

Regression Equation

Compressive strength (MPa) = -72.61 + 7.88 Nozzle Diameter (mm) + 0.1275 Printing speed (mm/sec) + 22.50 Layer thickness (mm) + 0.3925 Nozzle temperature (^{0}C)

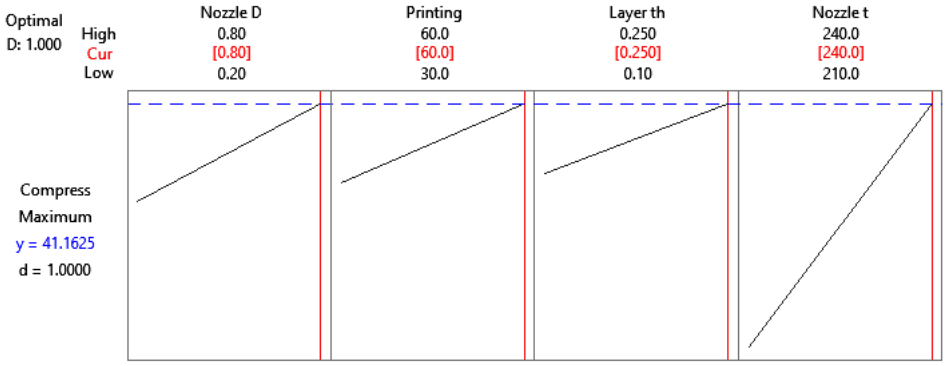

Figure-4. Compressive strength analysis via optimizer plot.

Figure-4 presented the optimizer plot for compressive strength analysis. This optimizer plot represents the excellent correlation of 3D printing process parameters to attain the maximum compressive strength of the printed part. Based on the plot, the compressive strength reaches a maximum value of 41.1625 MPa by the way of influencing four parameters, namely diameter (0.80 mm), printing speed (60 mm/sec), layer thickness (0.250 mm), and nozzle temperature (240°C). All these are set to their highest levels within the investigated range. The upward trend in all graphs indicates that increasing the parameters enhances compressive strength. The desirability value, such as 1.0000, indicates that the selected settings are exactly optimized for this goal. Therefore, the plot visibly demonstrates that using high values of all four parameters records the excellent compressive strength.

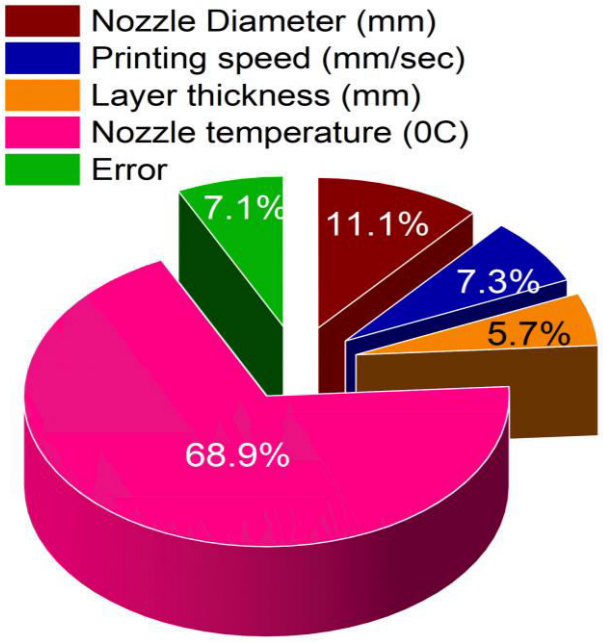

Figure-5. Compressive strength analysis by a pie chart.

Figure-5 represents the parameters' contribution through a pie chart. This analysis revealed that the nozzle temperature (68 %) highly effected in the compressive strength. Increasing temperature levels increase the melting point of the filament and offer uniform flow that forms excellent layers. Bonding of each layer provided good strength. The remaining parameters contributed to normal levels but offered good results.

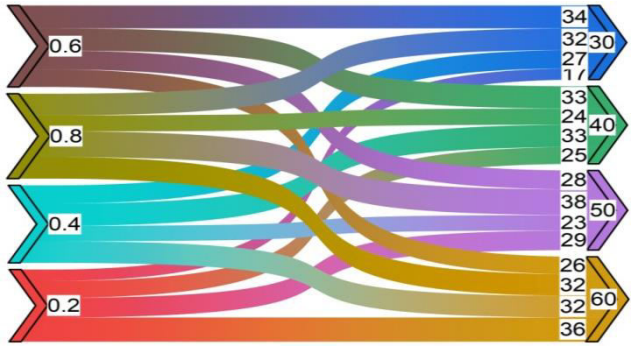

(a)

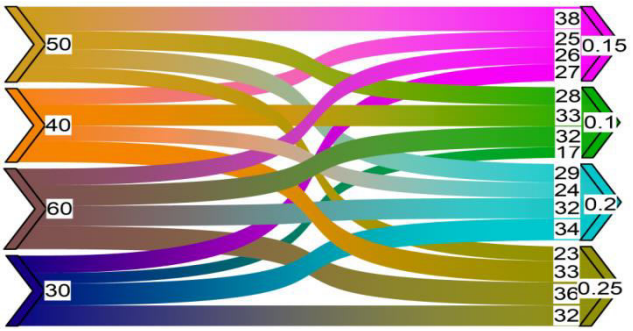

(b)

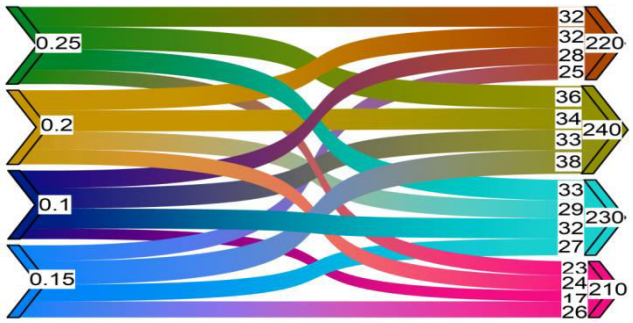

(c)

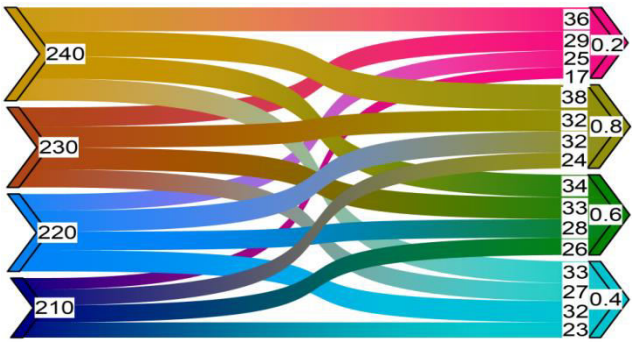

(d)

Figure-6. Relationship between FDM-3D printing parameters in developing Compressive strength on 3D-printed ABS-Carbon Fiber composite specimens through parallel set plots: (a) Nozzle diameter (mm) Vs Printing speed (mm/sec) (b) Printing speed (mm/sec) Vs Layer thickness (mm) (c) Layer thickness (mm) Vs Nozzle temperature (°C) (d) Nozzle temperature (°C) Vs Nozzle diameter (mm).

The interrelation between two process parameters was presented through a parallel set plot as shown in Figure-6. Two parameters, like nozzle diameter 0.8 mm and printing speed 50 mm/sec, correlation was recorded maximum compressive strength was recorded as shown in Figure-6 (a). The presented set illustrates that the size of the nozzle and the printing speed, in some way, affect the strength and stiffness of 3D-printed ABS Carbon Fiber components. Using a Sankey diagram, this map traces how the flow from nozzles of 0.2 mm, 0.4 mm, 0.6 mm, and 0.8 mm happens, leading to printing speeds between 30 mm/sec and 60 mm/sec. Each grouping of nozzle diameter with printing speed is a special combo, with the size of the bands showing the importance or frequency of that set. It is clear from the plot that using 0.6 mm and 0.8 mm nozzle diameters means printing can happen faster, at 40 and 50 mm/sec, since larger nozzles require more material to be released at the same time. Alternatively, 0.2 mm nozzles are used for both slow and fast printing, illustrating a need to discover how tiny layers are printed and how the system responds. The 0.4 mm nozzle seems to be chosen when aiming for a balance between refined detail and not wasting too much time. Ultimately, the visuals make it easier to choose the right nozzle diameter and speed combinations for nicely manufactured and strong composite samples. Lower values of nozzle diameter and printing speed decreased the compressive strength of the parts. Similarly, other parallel set plots could be understood.

A combination of printing speed 50 mm/sec and layer thickness 0.15 mm recorded excellent strength of the components as shown in Figure-6 (b). Minimum values of printing speed 30 mm/sec and layer thickness of 0.1 mm destroyed the strength of the components. Correlation between minimum layer thickness 0.15 mm and higher nozzle temperature 240 °C recorded good compressive strength; it was illustrated in Figure-6 (c). On the contrary, minimum compressive strength was found by the correlation of minimum levels of layer thickness 0.1 mm and nozzle temperature 210 °C. Interrelation between nozzle temperature 240 °C and nozzle diameter 0.8 mm recorded as excellent compressive strength of the parts as shown in Figure-6 (d). On the other hand, minimum compressive strength was found at minimum levels of nozzle temperature 210 °C and nozzle diameter 0.2 mm.

4.2 Surface Roughness Analysis

The " Smaller is better condition was selected in the surface roughness analysis; all the parameters' contributions with their levels were presented in Table-6. Based on the delta values and rank order, the influence of parameters was examined, and also found to be the most significant parameter in the surface roughness analysis. Comparing all four parameters, the nozzle diameter is the key parameter to modify the surface roughness, and it was noted as the priority, like first rank. Then the second priority of the parameter was found as layer thickness, followed by the third priority, which was nozzle

temperature. Finally, the fourth level of priority was recorded as printing speed. In the surface roughness analysis, the optimal parameters were found as 0.8 mm of nozzle diameter, 50 mm/sec of printing speed, 0.25 mm of layer thickness, and a nozzle temperature of 240°C. All parameters with higher values recorded minimum surface roughness values of the 3D printed parts.

Table-6. Surface roughness response table for signal to noise ratios.

Level	Nozzle Diameter (mm)	Printing speed (mm/sec)	Layer thickness (mm)	Nozzle temperature (^{0}C)
1	-9.375	-9.337	-9.356	-9.346
2	-9.255	-9.252	-9.274	-9.322
3	-9.246	-9.205	-9.234	-9.195
4	-9.145	-9.227	-9.159	-9.158
Delta	0.230	0.132	0.197	0.188
Rank	1	4	2	3

Surface roughness main effects plot for Means and S/N ratios was illustrated in Figure-7, which visibly identifies the parameters' influence in the surface roughness analysis. The parameter effects are also recorded in this plot, and easy way to reduce the surface roughness values of the 3D printed parts. Initially, all the parameters' values were transformed into Means and S/N ratio values, providing a clear orientation of their effect. The lower level of nozzle diameter, such as 0.2 mm, recorded high surface roughness; further increasing the nozzle diameter consistently reduced the surface roughness. Finally, increasing trends of the nozzle diameter up to 0.8 mm offered lower surface roughness of the parts. Consideration of printing speed, the lower level, such as 30 mm/sec, offered poor surface roughness, which leads to rejection of the parts, while in 3D printing. Then, increasing of the printing speed up to 50 mm/sec, the surface roughness of the printed parts was improved. Finally, the increasing trends of the printing speed from 50 mm/sec to 60 mm/sec, the surface roughness was varied, as the roughness increased. The lower level of layer thickness, like 0.1 mm, provided higher roughness values, further increasing the values from 0.1 mm to 0.25 mm, the surface roughness was excellent. Consideration of nozzle temperature, the higher nozzle temperature resulted in good surface roughness of the parts.

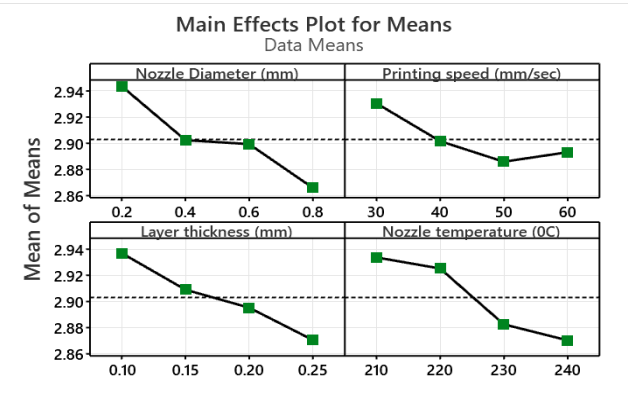

(a)

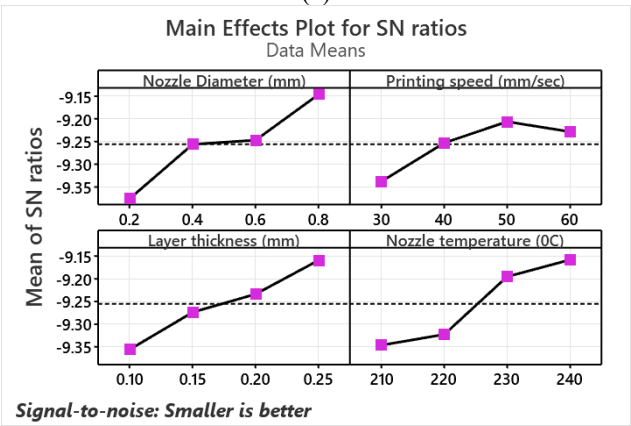

(b)

Figure-7. Surface roughness Main Effects plot: (a) Means and (b) S/N ratio.

According to the observations, having a nozzle diameter of 0.2 mm leads to increased surface roughness. It's mainly because the thin filament it uses can print precisely, but is also susceptible to vibrations, problems making extrusions, and variations in temperature. When the nozzle size rises to 0.8 mm, the strands print out thicker and more uniformly, so more of them cover the previous layer perfectly, smoothing out the result.

If printing slows down to 30 mm/sec, uneven thermal exposure and too much extrusion can lead to bad surface quality, sunken parts, and the 3D printing being rejected. An extrusion speed of nearly 50 mm/sec results in good surface smoothness because it matches the rate of moving the material with how quickly it solidifies. At speeds over 60 mm/sec, I notice that the roughness goes up again, which could happen if the layer is deposited at a speed too fast for the filament to lay smoothly.

A lower layer thickness means the printer must cross the same path more times, which increases the chance of roughness due to collected layer errors. A

change from 0.1 mm to 0.25 mm in layer thickness cuts down the number of layers, which means the material is deposited smoothly and consistently. To conclude, a higher temperature in the nozzle improves material flow and bonding, resulting in better interlayer fusing, even flow, and parts with superior surface quality. Taken together, these results highlight that setting FDM parameters correctly is necessary to achieve high-quality surfaces in printed pieces.

The normal probability plot explored the sixteen experimental runs' accuracy as shown in Figure-8. In the probability plot of surface roughness, all the data points commonly follow the exact straight line, which indicates a exactly good visual fit to a normal distribution. From the Anderson-Darling test, the yielded a P-value is 0.012, which is below the 0.05 threshold, so it indicates that the data statistically deviates from normality at the 5% significance level. The investigated mean surface roughness is exactly 2.903 microns, with a standard deviation of 0.05200, based on 16 trials. This plot represents 95% confidence interval, which is also through the green curves in the plot, and this supports a perfect estimation of the distribution parameters. Hence, this deviation will take appropriate statistical methods where normality assumptions are critical.

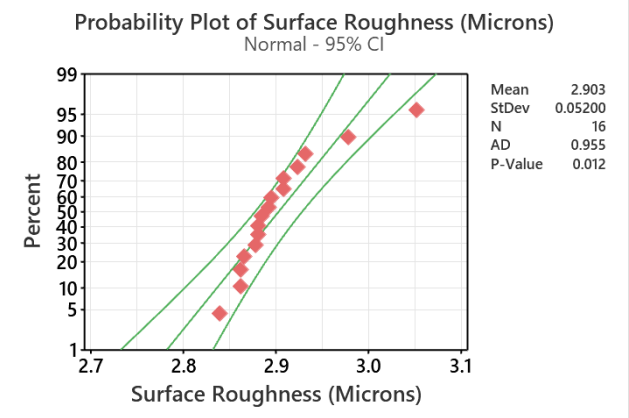

Figure-8. Normal probability plot for surface roughness analysis.

Detailed evaluation of the ANOVA analysis for surface roughness was tabulated in Table-7, which provided parameter effects in a detailed manner, like contribution percentage. This analysis, considering 95% confidence level, is like taking a P-value of 0.05. Mainly, the F-values and P-values played a vital role to examine the selected parameters were statistically significant or not, as all P-values lay below the 0.05 threshold value. In this analysis, all parameters P- value was lying below 0.05, so the conducted experimental work was appropriate.

Table-7. Surface roughness ANOVA analysis.

Source	DF	Seq SS	Contribution	Adj SS	Adj MS	F-Value	P-Value
Regression	4	0.034429	84.89%	0.034429	0.008607	15.44	0.000
Nozzle Diameter (mm)	1	0.011163	27.52%	0.011163	0.011163	20.03	0.001
Printing speed (mm/sec)	1	0.003290	8.11%	0.003290	0.003290	5.90	0.033
Layer thickness (mm)	1	0.009095	22.42%	0.009095	0.009095	16.32	0.002
Nozzle temperature (^{0}C)	1	0.010881	26.83%	0.010881	0.010881	19.52	0.001
Error	11	0.006130	15.11%	0.006130	0.000557		
Total	15	0.040559	100.00%				

Among all four parameters, three of them make nearly equal contributions in surface roughness analysis, except printing speed. In all parameters, the nozzle diameter contributed highly, like 27.52 %, followed by nozzle temperature, like 26.83 %, then layer thickness, 22.42 %. Finally, the printing speed contribution was recorded as 8.11 %. Nozzle diameter was extremely effective in the surface roughness modification in the 3D printed parts.

Regression Equation

Surface Roughness =3.619- 0.1181 Nozzle Diameter (mm) - 0.001283 Printing speed (mm/sec) - 0.426 Layer thickness (mm) - 0.002332 Nozzle temperature (^{0}C) Surface roughness performance metrics regression model is as follows: R-squared = 94.82%, Adjusted R-squared = 93.15%, and Predicted R-squared = 91.77%. All these values proved that the model has a powerful fit and good predictive capability. From this analysis, the equation exactly notices that all four process parameters, namely nozzle diameter, printing speed, layer thickness, and nozzle temperature, have a negative impact on surface roughness within the investigated range. In other words, an increase of any of these four parameters leads to a reduction in surface roughness, thereby enhancing surface quality.

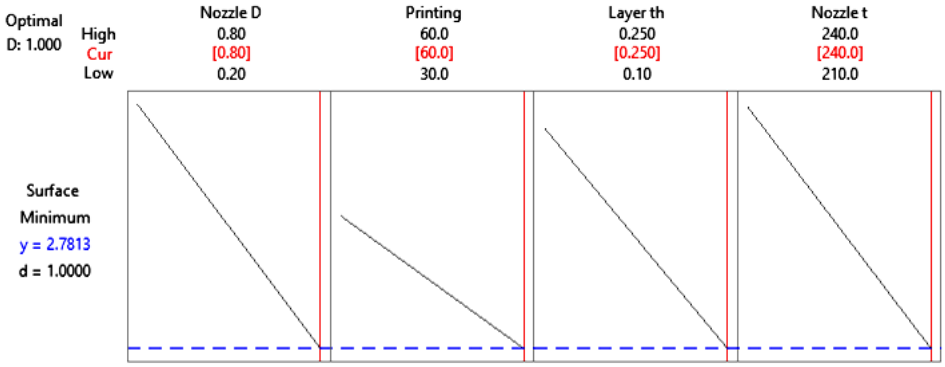

Figure-9. Optimizer plot for surface roughness analysis.

Figure-9 represents the optimizer plot for surface roughness analysis; the optimizer plot illustrates the ideal process settings to obtain the minimum surface roughness in 3D printing parts. The predicted minimum surface roughness value is 2.7813 microns, and the desirability value is 1.0000, which means the objective is exactly attained. The downward slope of all four graphs, such as nozzle diameter (0.80 mm), printing speed (60 mm/sec), layer thickness (0.250 mm), and nozzle temperature (240°C), denotes that increasing parameters highly reduce surface roughness. Hence, four parameters to their maximum values within the measured range result in the smoothest surface finish. This plot proves that higher values of these input parameters lead to excellent surface quality in the printed part.

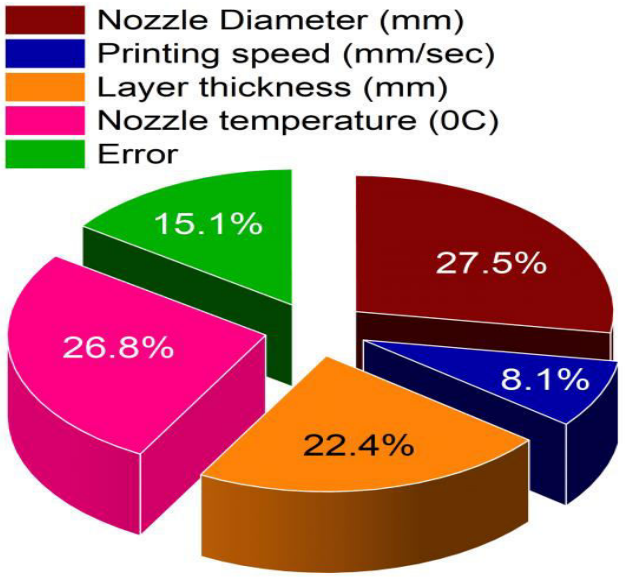

Figure-10. Pie chart for Surface roughness analysis.

Figure-10 presents the pie chart for surface roughness analysis and the microhardness analysis. From this analysis, the parameters' contribution percentage was clearly illustrated, and the maximum contribution was recorded as 27.5 % through nozzle diameter.

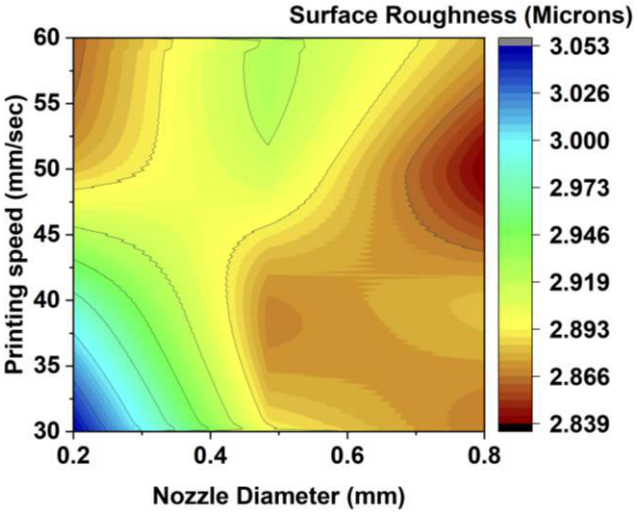

(a)

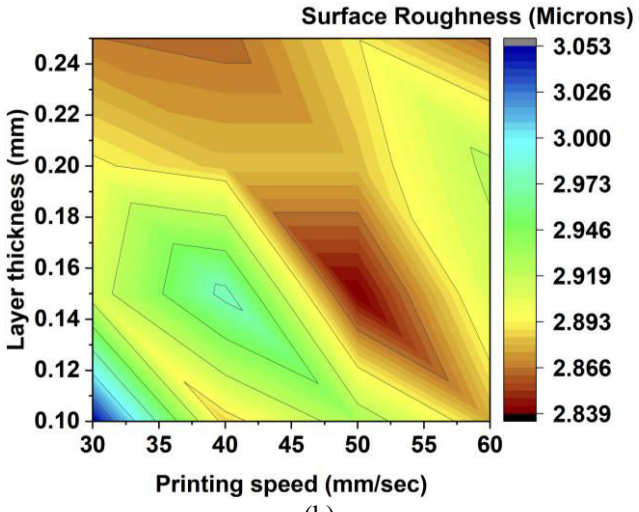

(b)

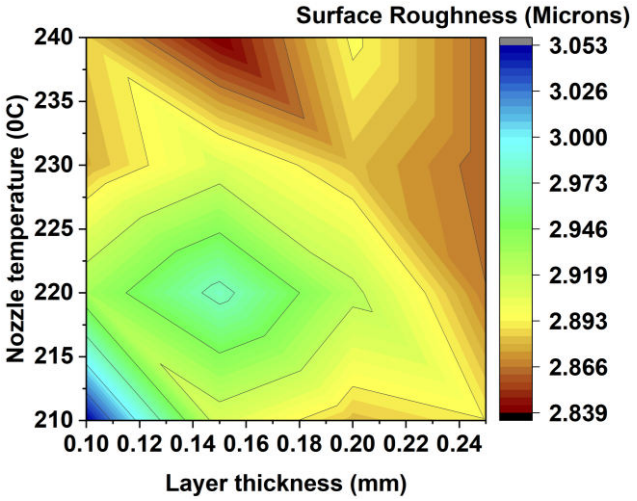

(c)

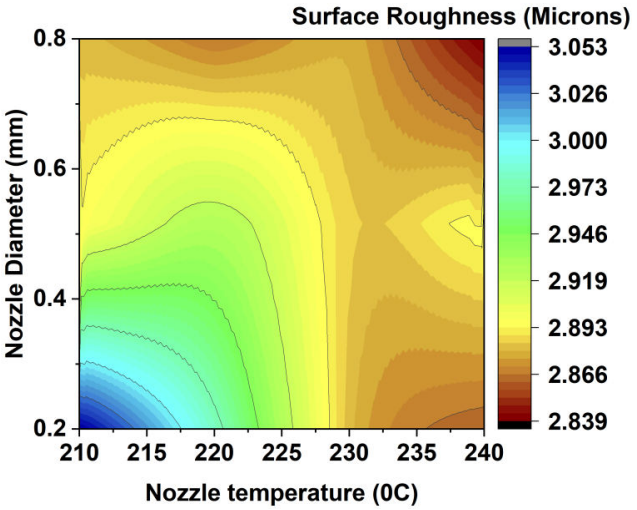

(d)

Figure-11. Surface roughness analysis through contour plot: (a) Nozzle diameter Vs. Printing speed (b) Printing speed Vs. Layer thickness (c) Layer thickness Vs. Nozzle temperature (d) Nozzle temperature Vs. Nozzle diameter.

The combination of parameter effects was illustrated in Figure-11 through a contour plot; this plot accurately showed the results with different parameter effects. Both lower levels of nozzle diameter and printing speed increase the surface roughness, whereas increasing both parameter levels reduces the surface roughness and offers a smooth surface, as shown in Figure-11(a). Similarly, both parameter minimum values, like printing speed and layer thickness, provided more surface roughness on the surface of the printed parts. On the other hand, moderate and increasing levels of parameters decrease the surface roughness and offer a good finish as shown in Figure-11(b). A combination of lower values of layer thickness and nozzle temperature increased the surface roughness; further increasing parameter values reduces the surface roughness, as shown in Figure-11(c). Higher values of nozzle diameter and nozzle temperature offered excellent smoothness of the 3D printed parts; it was illustrated in Figure-11(d). In this analysis, all the parameters with maximum values influence the recorded minimum surface roughness.

FDM 3D-printed components that were developed with hybrid ABS, carbon fiber composites, and optimized here reveal good potential for many applications because of their strong compression (38 MPa) and fine surface finish (2.839 µm). As a result, the material is ideal for building prototypes of strong parts in automotive and aerospace, where good strength, accuracy, and appearance are vital. Having carbon fiber reinforced allows brackets, housings, and mechanical connectors to be both strong and lightweight. The material is designed for use in manufacturing tools such as jigs, fixtures, and custom equipment, given that they require difficult and repeated use. For lightweight enclosures, parts of UAVs and drones, and robotic arms, the combination of smoothness and strength in the hybrid composite is key. Thanks to its ability to match precisely molded parts for each patient, additive manufacturing helps design useful implants, prosthetic legs and arms, wheelchairs, and various orthotic devices. In addition, the material is often used in motorsports and engineering because it supports aerodynamic design and forms strong, light support structures inside vehicles. Because of the optimized parameters, including a 0.8 mm nozzle diameter, 50 mm/sec printing speed, 0.15 mm layer thickness, and 240°C nozzle temperature, the parts retain their structural strength and still have surface quality. The production of these parts can be done efficiently, so they fit well with both manufacturing custom parts in small quantities and prototype creation. In general, hybrid ABS, carbon fiber FDM-printed plastic is flexible and can provide numerous advantages in areas that prioritize top performance, high precision, and being lightweight.

Increasing the strength and surface finish of bi-layered ABS, carbon fiber 3D printed parts can greatly improve their value for different engineering applications and help promote sustainability. As a result of this study, organizations can make resource-saving and durable composite parts, in line with international goals for lower waste and new materials. According to related sources, mixing natural fibers and nanomaterials is already supporting the development of eco-friendly composites that resist bacteria and have enhanced strength, and artificial intelligence is now guiding the process of finding the best parameters to boost their performance [47, 48]. In addition, turning lignin from jackfruit perianths into a valuable material highlights the focus on making material choices more sustainable [49]. By improving how hybrid materials are used through careful FDM control, this work supports this new area and offers choices for manufacturing that are eco-friendly, scalable, and suitable for industries such as healthcare and aerospace, while using fewer conventional, non-renewable resources.

5. CONCLUSIONS

This experimental work aimed to make hybrid layered 3D printed parts with additive manufacturing that was successfully conducted using two filaments, namely Acrylonitrile Butadiene Styrene (ABS) and composite materials, namely carbon fiber filaments. 3D printing parameters were optimized with the help of Taguchi optimization, and excellent outcomes, such as compressive strength and surface roughness, were obtained. Lastly, the results of this investigation were drawn as follows:

- From the compressive strength analysis, the maximum compressive strength of 38 MPa was recorded with a 0.8 mm nozzle diameter, 50 mm/sec printing speed, 0.15 mm layer thickness, and a nozzle temperature of 240°C. Among all the process parameters, nozzle temperature exhibited and recorded the highest influence with a contribution of 68.86%, followed by nozzle diameter of 11.09%, printing speed of 7.27%, and layer thickness of 5.66%. The experimental results clearly indicate that extreme nozzle temperatures significantly improve the compressive strength, primarily based on the enhanced interlayer bonding and fusion of the filament material during deposition.

- In the surface roughness analysis, revealed that the optimal parameter combination for attaining the lowest surface roughness is through a 0.8 mm nozzle diameter, 50 mm/sec printing speed, 0.25 mm layer thickness, and a nozzle temperature of 240°C. Notably, extreme levels of all parameters contributed to enhancing the surface finish by reducing the roughness of the 3D printed parts. Consideration of parameter influence, nozzle diameter emerged as the most significant factor, which is contributing 27.52% to alter the surface roughness, followed by nozzle temperature 26.83%, layer thickness 22.42%, and printing speed 8.11%. A strong dominant influence, namely nozzle diameter, enlightens its critical role in defining the extrusion path and material flow levels. This directly reflects the surface quality of the 3D printed parts.

REFERENCES

[1] Saharudin M. S., Hajnys J., Kozior T., Gogolewski D. and Zmarzły P. 2020. Quality of Surface Texture and Mechanical Properties of PLA and PA-Based Material Reinforced with Carbon Fibers Manufactured by FDM and CFF 3D Printing Technologies. Polymers, 13(11): 1671. https://doi.org/10.3390/polym13111671

[2] Kafshgar A. R., Rostami S., Aliha M., Berto F. 2021. Optimization of properties for 3D printed PLA material using Taguchi, ANOVA, and multi-objective methodologies. Procedia Struct Integr. 34: 71-77.

[3] León-Becerra J., González-Estrada O. A., Quiroga J. 2021. Effect of relative density on in-plane mechanical properties of common 3D-printed polylactic acid lattice structures. ACS Omega. 6: 29830-29838.

[4] Ansari A. A., Kamil M. 2022. Izod impact and hardness properties of 3D printed lightweight CF-reinforced PLA composites using design of experiment. Int J Light Mater Manuf. 5: 369-383.

[5] Agarwal K. M., Shubham P., Bhatia D., Sharma P., Vaid H. and Vajpeyi R. 2021. Analyzing the Impact of Print Parameters on Dimensional Variation of ABS specimens printed using Fused Deposition Modelling (FDM). Sensors International, 3, 100149. https://doi.org/10.1016/j.sintl.2021.100149

[6] Dave H. K., Prajapati A. R., Rajpurohit S. R. *et al*. 2022. Investigation on tensile strength and failure modes of FDM printed part using in-house fabricated PLA filament. Adv Mater Process Technol. 8: 576-597.

[7] Maguluri N., Suresh G., Rao K. V. 2023. Assessing the effect of FDM processing parameters on the mechanical properties of PLA parts using the Taguchi method. J Thermoplast Compos Mater. 36: 1472-1488.

[8] Frunzaverde D., Cojocaru V., Bacescu N., Ciubotariu C. 2023. The influence of the layer height and the filament color on the dimensional accuracy and the tensile strength of FDM-printed PLA specimens. Polymers (Basel). 15(10): 2377.

[9] El M. A., El Mabrouk K., Vaudreuil S., Touhami M. E. 2019. Mechanical properties of CF-reinforced PLA parts manufactured by fused deposition modeling. J Thermoplast Compos Mater. 34: 581-595.

[10] Maqsood N. and Rimašauskas M. 2021. Characterization of carbon fiber reinforced PLA composites manufactured by fused deposition modeling. Composites Part C: Open Access, 4, 100112. https://doi.org/10.1016/j.jcomc.2021.100112

[11] Auffray L., Gouge P. A., Hattali L. 2022. Design of experiment analysis on tensile properties of PLA samples produced by fused filament fabrication. Int. J Adv Manuf Technol. 118: 4123-4137.

[12] Ambade V., Rajurkar S., Awari G. *et al*. 2025. Influence of FDM process parameters on tensile strength of parts printed by PLA material. Int. J Interact Des Manuf 19, 573-584. https://doi.org/10.1007/s12008-023-01490-7

[13] Brackett J., Cauthen D., Condon J. *et al*. 2022. The impact of infill percentage and layer height in small-scale material extrusion on porosity and tensile properties. Addit Manuf. 58: 103063.

[14] Hikmat M., Rostam S., Ahmed Y. M. 2021. Investigation of tensile property-based Taguchi method of PLA parts fabricated by FDM 3D printing technology. Results Eng. 11: 100264.

[15] Taborda-Ríos J. A., López-Botello O., Zambrano-Robledo P. *et al*. 2020. Mechanical characterisation of a bamboo fibre/polylactic acid composite produced by fused deposition modelling. J Reinf Plast Compos. 39: 932-944.

[16] Saleh M., Anwar S., M A. and Al Faify A. Y. 2022. Prediction of Mechanical Properties for Carbon Fiber/PLA Composite Lattice Structures Using Mathematical and ANFIS Models. Polymers, 15(7): 1720. https://doi.org/10.3390/polym15071720

[17] Yang T. C., Yeh C. H. 2020. Morphology and mechanical properties of 3D printed wood fiber/polylactic acid composite parts using fused deposition modeling (FDM): the effects of printing speed. Polymers (Basel). 12: 1334.

[18] Dou H., Cheng Y., Ye W., Zhang D., Li J., Miao Z., and Rudykh S. 2019. Effect of Process Parameters on Tensile Mechanical Properties of 3D Printing Continuous Carbon Fiber-Reinforced PLA Composites. Materials, 13(17): 3850. https://doi.org/10.3390/ma13173850

[19] Ali S., Abdallah S., Devjani D. H. *et al*. 2022. Effect of build parameters and strain rate on mechanical properties of 3D printed PLA using DIC and desirability function analysis. Rapid Prototyp J. 29: 92-111.

[20] Zonoobi M. A., Haghshenas Gorgani H., and Javaherneshan D. 2023. Experimental investigation and multi-objective optimization of FDM process parameters for mechanical strength, dimensional accuracy, and cost using a hybrid algorithm. Scientia Iranica, (), -. doi: 10.24200/sci.2023.60960.7090

[21] Fischer D., Eßbach C., Schönherr R., Dietrich D. and Nickel D. 2022. Improving inner structure and properties of additive-manufactured amorphous plastic parts: The effects of extrusion nozzle diameter and layer height. Additive Manufacturing, 51, 102596. https://doi.org/10.1016/j.addma.2022.102596.

[22] Gebisa A. W., Lemu H. G. 2018. Investigating Effects of Fused-Deposition Modeling (FDM) Processing Parameters on Flexural Properties of ULTEM 9085 using Designed Experiment. Materials. 11(4): 500. https://doi.org/10.3390/ma11040500

[23] Luzanin O., Guduric V., Ristic I., and Muhic S. 2017. Investigating the impact of five build parameters on the maximum flexural force in FDM specimens - a definitive screening design approach. Rapid Prototyping Journal, 23(6): 1088-1098. https://doi.org/10.1108/RPJ-09-2015-0116

[24] Kumar N. H., Adarsha H., Keshavamurthy R., and Kapilan N. 2024. Influence of carbon nano fibre addition on the mechanical behaviour of PLA-based 3D printed polymer nano composites. Journal of the Institution of Engineers (India): Series D. 105(1): 33-47.

[25] Tura A. D. and Mamo H. B. 2022. Characterization and parametric optimization of the additive manufacturing process for enhancing mechanical properties. Heliyon, 8(7).e09832. https://doi.org/10.1016/j.heliyon.2022.e09832

[26] Pagés-Llobet A., Espinach F. X., Julián F. *et al.* 2023. Effect of extruder type in the interface of PLA layers in FDM printers: filament extruder versus direct pellet extruder. Polymers (Basel) 15:2019.

[27] Kamaal, M., Anas, M., Rastogi, H. *et al*. 2021. Effect of FDM process parameters on mechanical properties of 3D-printed carbon fibre-PLA composite. Prog Addit Manuf 6, 63-69. https://doi.org/10.1007/s40964-020-00145-3

[28] Lee C. H., Padzil F. N. B. M., Lee S. H. *et al*. 2021. Potential for natural fiber reinforcement in PLA polymer filaments for fused deposition modeling (FDM) additive manufacturing: a review. Polymers (Basel). 13: 1407.

[29] Khalili A., Kami A., Abedini V. 2023. Tensile and Flexural Properties of 3D-Printed Polylactic Acid/Continuous Carbon Fiber Composite. Mech Adv Compos Struct. 10: 407-418.

[30] Ezzaraa I., Ayrilmis N., Kuzman M. K. *et al*. 2020 Study of the effects of microstructure on the mechanical properties of 3D printed wood/PLA composite materials by a micromechanical approach. In: 2020 IEEE 2nd International Conference on electronics, control, Optimization, and computer science, ICECOCS 2020.

[31] Arunkumar N., Sathishkumar N., Sanmugapriya S. S., Selvam R. 2021. Study on PLA and PA thermoplastic polymers reinforced with carbon additives by the 3D printing process. Mater Today Proc. 46: 8871-8879.

[32] Pazhamannil R. V., Govindan P., Edacherian A. *et al*. 2024. Impact of process parameters and heat treatment on fused filament fabricated PLA and PLA-CF. Int J Interact Des Manuf. 18, 2199-2213. https://doi.org/10.1007/s12008-022-01082-x

[33] Saad M. S., Mohd Nor A., Zakaria M. Z., Baharudin M. E., Yusoff W. S. 2021. Modelling and evolutionary computation optimization on FDM process for flexural strength using an integrated approach of RSM and PSO. Prog Addit Manuf. 6: 143-154.

[34] Chawla K., Singh J., Singh R. 2023. Mechanical investigations on secondary recycled ABS-based composite multi-layered tensile and flexural specimens prepared by fused filament fabrication. Prog Addit Manuf. 8: 1195-1208.

[35] Poier P. H., Arce R. P., Rosenmann G. C., Carvalho M. G. R., Ulbricht L., Foggiatto J. A. 2021. Development of modular wrist, hand, and finger orthoses by additive manufacturing. Res Soc Dev. 10: e333101522707.

[36] Thakur V., Kumar R., Kumar R., Singh R., and Kumar V. 2024. Hybrid additive manufacturing of highly sustainable Polylactic acid -Carbon Fiber-Polylactic acid sandwiched composite structures: Optimization and machine learning. Journal of Thermoplastic Composite Materials. https://doi.org/10.1177_08927057231180186

[37] Aslani K-E, Chaidas D., Kechagias J., Kyratsis P., Salonitis K. 2020. Quality performance evaluation of thin-walled PLA 3D printed parts using the Taguchi method and grey relational analysis. J Manuf Mater Process. 4: 47.

[38] Benwood C., Anstey A., Andrzejewski J. *et al*. 2018. Improving the impact strength and heat resistance of 3D printed models: structure, property, and processing correlationships during fused deposition modeling (FDM) of poly (lactic acid). ACS Omega. 3: 4400-4411.

[39] Kechagias J. D., Vidakis, N. 2022. Parametric optimization of material extrusion 3D printing process: an assessment of Box-Behnken vs. full-factorial experimental approach. Int J Adv Manuf Technol. 121: 3163-3172.

[40] Bhagia S., Lowden R. R., Erdman D. *et al*. 2020. Tensile properties of 3D-printed wood-filled PLA materials using poplar trees. Appl Mater Today. 21: 100832.

[41] Hanon M. M., Dobos J., Zsidai L. 2020. The influence of 3D printing process parameters on the mechanical performance of PLA polymer and its correlation with hardness. Procedia Manuf. 54: 244-249.

[42] Arunachalam S. J. and Saravanan R. 2024. Comprehensive Insights of Chemically Treated Jute/Kenaf/Glass Fiber with TiO2 nanoparticle using RSM optimization. J. Environ. Nanotechnol. 13(2): 21-30.

[43] Khan I., Barsoum I., Abas M., Al Rashid A., Koç M. and Tariq M. 2024. A review of extrusion-based additive manufacturing of multi-material polymeric laminated structures. Composite Structures, 349-350, 118490. https://doi.org/10.1016/j.compstruct.2024.118490

[44] Khan I., Farooq U., Tariq M., Abas M., Ahmad S., Shakeel M., Riaz A. A. and Hira F. 2025. Investigation of effects of processing parameters on the impact strength and microstructure of thick tri-material-based layered composite fabricated via extrusion-based additive manufacturing. Journal of

Engineering Research. 13(1): 243-250. https://doi.org/10.1016/j.jer.2023.08.007

[45] Khan I., Rasheed A., Khan M. *et al*. 2025. Investigation and Optimization of Processing Parameters Affecting the Mechanical Properties of Carbon Particle-Reinforced Thermoplastic Polyurethane Samples Fabricated via Fused Filament Fabrication. J. of Materi Eng and Perform. https://doi.org/10.1007/s11665-025-11154-0

[46] Abas M., Habib T., Khan I. *et al*. 2025. Definitive screening design for mechanical properties enhancement in extrusion-based additive manufacturing of carbon fiber-reinforced PLA composite. Prog Addit Manuf. 10, 139-157. https://doi.org/10.1007/s40964-024-00610-3

[47] Lakshmaiya N., Karthick M., Bhaskar K., Chukka N. D. K. R., Ross N. S., and Maranan R. 2025. Development of Eco-Friendly Hybrid Nanocomposites with Improved Antibacterial and Mechanical Properties through NaOH-Treated Natural Fibers. Results in Engineering. p. 104996

[48] Lakshmaiya N., Chukka N. D. K. R., Kaliappan S., Balaji V., Ross N. S., and Maranan R. 2025. An integrated artificial neural network technique to optimize the various parameters of Pineapple/SiO2/epoxy-based nanocomposites under NaOH treatment. Results in Engineering. 26, p. 104737.

[49] Natrayan L., Kaliappan S., Okla M. K., Josphineleela R., and Iqbal A. 2024. Extraction of lignin from fluorescent perianths of jack fruit and its mechanical, wear, creep, and flammability behaviour of abaca-polyester composites. Waste and Biomass Valorization. 15(10): 5887-5898.